Port Function Based Modeling and Control of an Autonomously Variable Spring to Suppress Self-Excited Vibrations While Drilling

Stephen P. Buerger, Mikhail Mesh, David W. Raymond

***Abstract*— Self-excited vibrations are a major problem for rotary drilling. They may be mitigated by introducing adjustable compliance near the bottom of the drillstring, but it is challenging to identify the appropriate stiffness, particularly in situ and with limited available data on the rapidly-changing overall system dynamics. We describe an approach to modeling and simulating self-excited vibrations in drillstrings. Our approach uses impedance and admittance port functions to represent and systematically combine subsystems, and integrates established models for drillstring vibrations and rock / bit interactions. Simulations predict that intermediate stiffnesses provide better stability than either compliant or stiff extremes, which aligns with results from earlier work. Results also indicate that at least two different mechanisms limit stability in different stiffness regimes, producing significant differences in the relationship between vibration frequency and controlled module stiffness. This suggests a potential means of developing autonomous stiffness controllers that depend only on measurements taken at the variable stiffness module, without requiring a dynamic model of the rest of the drillstring.**

I. Introduction

Drillstring vibrations can cause ineffective drilling and equipment damage and are a leading cause of non-productive time in the drilling industry [1,2]. As hole depth increases, the drillstring becomes increasingly compliant and interacts with the large mass near the bit to create multiple modes of vibration across a wide range of frequencies. The lower right pane of Fig. 1 depicts the root cause of self-excited longitudinal vibrations. Cutter forces at the rock/bit interface are modulated by the dynamic response of the bit and drillstring, producing a variable cutting force that can self-excite the modes of vibration of the drillstring. Conceptually, successive periodic passes of the bit over the uneven bottom-hole surface act as an effective delay, introducing the possibility of instability [3].

Numerous approaches to suppressing vibrations have been explored, including tailoring the bit design to specific drilling conditions [4], monitoring and suppressing chatter via machine learning and spindle speed control [5], and impact dampers [6]. None of these approaches accommodate highly variable drillstring dynamics.

Dynamic elements may be used to limit the transmissibility between the bit forces and the drillstring,

This research was funded by the Laboratory Directed Research and Development (LDRD) program at Sandia National Laboratories.

The authors are with Sandia National Laboratories, Albuquerque, NM 87185 USA (S.P.B. phone: 505-284-3381; emails: {sbuerge | dwraymo | mmesh}@sandia.gov)

Sandia National Laboratories is a multi-mission laboratory managed and operated by Sandia Corporation, a wholly owned subsidiary of Lockheed Martin Corporation, for the U.S. Department of Energy's National Nucledar Security Administration under contract DE-AC04-94AL85000.

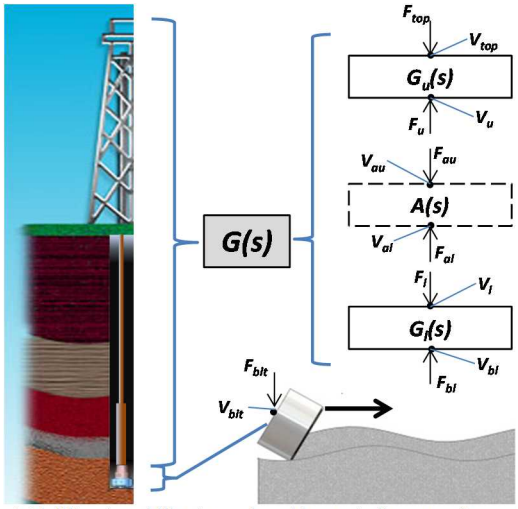

Figure 1. Drilling instability is produced by periodic cutter forces self-exciting drillstring modes of vibration.

reducing instability. However, the drillstring dynamics vary dramatically as holes are drilled, as a result of: adding drill pipe, frictional interaction and jamming between the drill pipe and the wellbore, and other factors. Furthermore, the rock-bit interaction characteristics change with different drilling conditions, e.g. different layers of rock as shown in Fig. 1 (left). Because of this variability, it is virtually impossible to specify a single set of dynamic parameters to prevent all unstable vibrations. Therefore, tunable dynamic elements have been used. In prior work, variable dampers were used to suppress vibrations. However, this work revealed that varying the stiffness of an element close to the bit also had a strong effect on vibration [7].

We are developing drillstring modules with controllable stiffness to actively suppress drillstring vibrations [8]. In theory, by introducing compliance that is controllable over a broad range, most or all unstable self-excited vibrations may be suppressed. However, several factors make the control of stiffness challenging. First, the overall drillstring dynamics are very challenging to observe from any one location (e.g. the surface). Second, given the challenges of drillstring telemetry, variable stiffness modules must be autonomously controlled based on local sensor measurements. Third, the rock-bit interactions contribute not only excitation forces but also coupled dynamics based on elastic and dissipative behavior that depends on the drilling medium and the bit. These dynamics are very difficult to characterize, making some of the key system dynamics effectively unobservable.

Before autonomous downhole controllers may be developed, it is necessary to establish a modeling and simulation capability to understand and analyze drillstring behavior. Fig. 1 illustrates a generic representation of drillstring dynamics with an adjustable module. The

dynamics of the overall drilling system as it appears at the bit may be represented by the Laplace domain transfer function *G(s)*. *G(s)* may be decomposed by dynamic substructuring [9] into a controllable "actuator" portion (e.g. a variable spring) *A(s)*, and portions of the drillstring that are below ($G_l(s)$) and above ($G_u(s)$) the actuator. Forces *F* and velocities *V* at subsystem interfaces are indicated. Partitioning the system in this manner enables analysis based on the forces and motion exchanged between the controllable actuator and the uncertain drillstring dynamics. It also allows simulations to be rapidly iterated by changing *A(s)* without needing to recalculate $G_l(s)$ or $G_u(s)$.

In Section II we present a substructured modeling approach for drillstrings with actively controlled elements based on the use of port functions. This model combines prior work in drillstring instability modeling with a widely accepted model for rotary drag bit drilling. In Section III we present the results of simulations that explore the stability properties of the coupled system for a simplified drillstring model with different series stiffness values. In Section IV we explore the implications of these simulation results for local autonomous stiffness control methods, sketching out a potential approach that depends only on directly measured local information. Section V provides discussion and conclusions, including a description of key future work.

II. Dynamic Modeling

A novel model, suitable for study of the instability / self-excited vibration problem, was developed by compiling four key techniques: subsystems were modeled using finite element representations, then combined using port functions, the cutting force instability model of [3] was implemented, and instantaneous rock/bit interaction forces were calculated by applying a physics-based model [10,11]. This section summarizes these elements.

A. Drillstring Subsystem Models

We have developed several means of representing complex drillstring subsystems via finite element methods. Primarily, drillstring structural dynamics models have been reproduced using discretization of spring-mass systems into a normal modes model implemented in MATLAB. Results were validated by comparing to an identical model implemented in MSC Nastran and by comparing to earlier published data [8,12]. This model synthesis method was applied to a 7200 ft drillstring common in the literature [3], as well as to alternative models up to 16,000 ft in length [8]. (English units are used as is standard in the drilling industry and literature.) This is our primary method for generating models for the $G_l(s)$ and $G_u(s)$ blocks in Fig. 1.

B. Dynamic Substructured Model using Port Functions

Substructuring methods were used to explore different dynamic topologies for controllable "actuator" elements (*A(s)* in Fig. 1) without needing to derive new equations or develop new finite element models for the full system each time the dynamics change. Specifically, the port functions *mechanical impedance* and its inverse, *mechanical admittance*, were chosen to represent each subsystem because they provide several advantageous properties. Mechanical impedance is defined as the force produced in response to an imposed velocity, and characterizes the static and dynamic behavior of the system at a particular spatial location or *port of interaction* [13]. Because impedance and admittance are defined in terms of power conjugate variables (force and velocity), they enable analytical methods that are not impacted by the instantaneous direction of energy flow. They also seamlessly handle connection of multiple subsystems without the need to consider impedance matching or loading by other subsystems (unlike other analytical methods such as block diagrams). Fundamentally this distinction is because port functions represent the dynamic behavior of systems as observed at a single point of interaction with other systems – as opposed to "forward path" representations (e.g. block diagrams) that relate an output at one physical location to an input somewhere else. Furthermore, this construct enables the explicit *control* of port function behavior, potentially enabling application of impedance control [14] to the controllable module.

Our approach represents the drillstring as a series of impedance and admittance functions, alternating in causality. Terminating (top and bottom) elements in the string may be represented as single-port functions, whereas intermediate subsystems are represented as "two-port" functions that interact both above and below. Subsystems may include arbitrary dynamic order and complexity, and can be linear or nonlinear, time-varying or invariant. Details for deriving port functions from normal mode coefficients are provided in section 2.3 of [8].

C. Instability Model

A theory of instability in machining developed by Tlusty is presented in [15] and its application to the drilling vibration problem is described in [3]. This work elucidates the interactions between the drillstring, drill bit, and drilling medium, and the quantitative roles that each play in determining susceptibility to self-excited vibrations. Limiting conditions are found that define the conditions under which stability may and may not be guaranteed. First, a limiting bit diameter is derived. At smaller diameters, the system is stable, whereas at larger diameters instability is possible if problematic frequencies are excited. Thus the bit diameter defines a boundary that can be used to quantify the relative stability as dynamics are changed. Second, it is determined that by making the real portion of the transfer function from bit force to bit displacement positive at frequencies of potential vibration, the contribution of those frequencies to self-excited vibrations can be eliminated. Thus a design goal for vibration absorbers is to "lift" the real portion of the transfer function at problematic frequencies, making them positive or, at least, less negative [3].

We apply and extend this model to include a widely-used model for rock/bit interaction and explore system-level simulations to predict the onset of actual unstable vibrations (rather than simply the susceptibility to *potential* instability). We also apply the key conclusions from this prior work in seeking methods to autonomously sculpt the controllable stiffness to minimize self-excited vibration instabilities.

D. Rock/Bit Interaction Forces

Rather than the simplified model for rock/bit interaction used in [3], we incorporate the widely accepted friction-based model of Detournay [10,11]. A complete model to predict the force, torque, and displacements inherent to the rock-bit

interaction process is provided in [11]. Since we are only concerned with longitudinal forces and displacements, we apply Detournay's model only to compute the reaction force F_{bit} in response to a specific depth of cut d at a specified constant angular velocity ω, assuming that the drilling system can provide the requisite torque to maintain that velocity.

Drilling processes are characterized by three regions associated with increasing applied force or weight on bit: Region 1, in which the cutters are not fully engaged with the rock; Region 2, in which the cutters are fully engaged and increasing weight on bit results in linearly increasing depth of cut; and Region 3, in which one of several drilling pathologies occurs, e.g. the depth of cut reaches the maximum physical cutter depth, resulting in reduced drilling performance [16]. For this analysis, we restrict study to Region 2, where productive drilling occurs.

Detournay's model defines the relationships between the scaled weight on bit (w) and scaled depth of cut (d) in equation 4 in [11]:

$$w = \frac{F_{bit}}{a}, \quad d = \frac{2\pi V_{bit}}{\omega} \tag{1}$$

We assume that the bit has full cross section with radius a. $V_{bit} = \dot{Z}_{bit}$ is the linear bit velocity or rate of penetration. The values for w and d at the onset of Region 2 (the transition from Region 1) are defined as w_* and d_*. In Region 2, equation 37 in [11] relates w and d:

$$w = \zeta\varepsilon(d - d_*) + w_* \tag{2}$$

ζ and ε are two constants, specific to rock and bit, that define the cutting process. In brief, ε is the energy required to remove a unit volume of rock by an ideally sharp bit, and ζ characterizes aspects of the bit. Equation (2) shows that the reaction force includes a spring-like portion that is proportional to the depth of cut, plus a Coulomb friction component represented by w_*. Together, (1) and (2) enable the computation of the force F_{bit} in response to a linear velocity V_{bit}, at a particular angular velocity ω. This provides an impedance representation of the rock/bit interactions.

III. Simulations

This model was implemented in MATLAB and Simulink to enable rapid parametric simulations. These simulations were used to study the impact of changes in the variable stiffness on the stability properties of the system and the emergence of self-excited vibrations. Furthermore, the characteristics of unstable vibrations at the stability boundaries were used to provide insight into the nature of the instabilities, suggesting potential methods for autonomously controlling the down-hole vibration suppression system.

A. MATLAB / Simulink Implementation

The integrated longitudinal vibration model was simulated in MATLAB and Simulink. A block diagram of the substructured drillstring model is shown in Fig. 2. There are four major system elements, each represented by port functions: the upper drillstring, the actuator or variable spring, the lower drillstring (between the variable spring and the point of contact with the rock), and the rock/bit interactions. To enforce proper causality, alternating impedance / admittance representations were used: the upper and lower drillstrings were represented with admittance

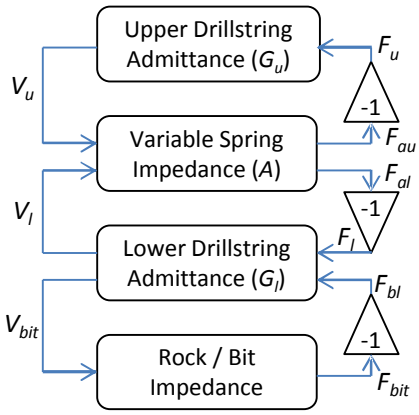

Figure 2. Block diagram of port-function based drillstring model.

functions, and the actuator and rock/bit interactions with impedance functions. The terminating subsytems - rock/bit interactions and the upper drillstring - were represented with single-port functions, whereas the intermediate elements were represented with two-port functions.

Simulations were conducted using a normal modes representation of the 7200 ft drillstring described in [3], to prove accuracy of the model with complex drillstrings. A simplified model, a 2nd order simple harmonic oscillator (SHO) was also simulated and studied in greater detail to align with previous experimental studies [7] and to enable more intuitive understanding of the primary subject of interest: the interactions between the model elements, including between the Detournay rock-bit interaction model [11] and the Tlusty model for instability [3]. Prior work has shown the utility of reduced-order models ranging from 1 to 6 modes in studying drillstring vibrational instabilities [3,7].

In the case of the SHO drillstring, the upper drillstring admittance is represented in the Laplace domain as:

$$G_u = \frac{V_u}{F_u} = \frac{s}{m_u s^2 + b_u s + k_u} \tag{3}$$

The SHO includes a mass m_u=1613 *lb*, stiffness k_u=5500 *lb/in*, and damping ratio tuned to 0.4 via the damping coefficient b_u. The lower drillstring is a two-port admittance representation of a rigid mass m_l=180 *lb*:

$$\begin{bmatrix} V_l \\ V_{bl} \end{bmatrix} = G_l \begin{bmatrix} F_l \\ F_{bl} \end{bmatrix} = \begin{bmatrix} \frac{1}{m_l s} & \frac{1}{m_l s} \\ \frac{1}{m_l s} & \frac{1}{m_l s} \end{bmatrix} \begin{bmatrix} F_l \\ F_{bl} \end{bmatrix} \tag{4}$$

The actuator is represented as a two-port impedance consisting of a parallel spring with variable stiffness k_{vs} and damper b_{vs} per the matrix equation:

$$\begin{bmatrix} F_{au} \\ F_{al} \end{bmatrix} = A \begin{bmatrix} V_{au} \\ V_{al} \end{bmatrix} = \begin{bmatrix} \frac{b_{vs}s + k_{vs}}{s} & -\left(\frac{b_{vs}s + k_{vs}}{s}\right) \\ -\left(\frac{b_{vs}s + k_{vs}}{s}\right) & \frac{b_{vs}s + k_{vs}}{s} \end{bmatrix} \begin{bmatrix} V_{au} \\ V_{al} \end{bmatrix} \tag{5}$$

For each value of k_{vs}, b_{vs} was tuned to provide a damping ratio of 0.4 for the mode created by the mass m_l and k_{vs}.

The rigid connection of subsystems yields:

$$V_u = V_{au}, \quad V_l = V_{al}, V_{bit} = V_{bl} \tag{6}$$

Enforcing Newton's second law requires equal and opposite forces at the interfaces:

$$F_u = -F_{au}, \quad F_l = -F_{al}, F_{bit} = -F_{bl} \tag{7}$$

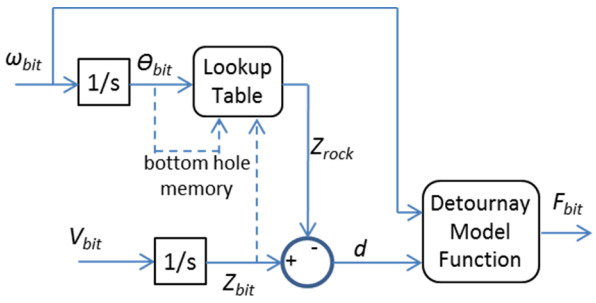

Figure 3. Implementation of rock-bit interaction model

Finally, the rock/bit interactions are represented in impedance form by applying (1) and (2). A block diagram of this algorithm is shown in Fig. 3. The angular coordinate is modeled to capture the position-dependent geometry of the hole bottom. The angular and vertical bit positions are determined by integrating the respective velocities. The current geometry of the bottom of the hole (height versus angle) is stored in a dynamic lookup table, which is updated by circular buffers (not shown). On each revolution, all material above the cutter is assumed to be removed, so that the difference in vertical bit position from one pass to the next is the depth of cut, *d*. (This model assumes that the bit stays in contact with the rock, which can be verified by studying F_{bit}.) The parameters ζ, ε, d^* and w^* are derived from literature or testing (for our example, coefficients were derived from testing in Sierra White Granite) and used to populate the Detournay model function. This function uses these parameters as well as *a*, *d,* and ω, and solves (1) and (2) for the instantaneous F_{bit}. To provide an initial excitation, the bottom hole is given a sinusoidal initial geometry.

Notably, each of the four blocks in Fig. 2 (and the corresponding relationships in (3)-(5) and Fig. 3) can be replaced with alternative models for different dynamics, enabling seamless, modular drillstring simulations. To our knowledge, this is the first implementation of the prevailing friction-based drag bit model of Detournay as a modular substructured port function suitable for simulation with common control systems design and analysis tools.

B. Stability vs. Stiffness

A series of simulations was run with several variable parameters to analyze the system's stability limits. Increasing the bit radius *a* makes unstable vibrations more likely by increasing the effective rock-bit stiffness (this is evident by substituting (1) into (2)). Therefore *a* is a useful parameter for defining the relative stability for different values of the variable stiffness. For a particular stiffness, a stability margin can be defined in terms of *a*, e.g. the difference between the actual and maximum stable values for *a*. As in [3], we present a stability boundary in terms of maximum stable *a* – in this case presented versus stiffness.

Because multiple modes of vibration are present, some potentially unstable and others stable, we define instability as occurring if vibrations are increasing in amplitude after 20 seconds from initial excitation. Examples of stable and unstable bit velocity profiles are shown in Fig. 4.

Simulations were conducted at values for k_{vs} ranging from 1500 to 50k *lb/in*. At each k_{vs} value, *a* was increased to find its maximum stable value. This process was repeated for three angular velocities ω in the typical range for rock

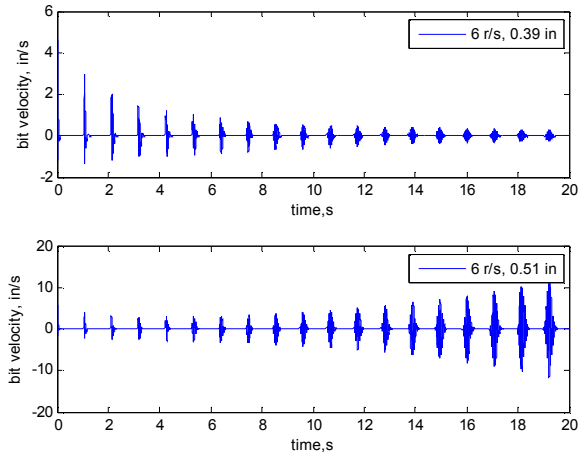

Figure 4. Stable and unstable velocity trajectories for a 6k *lb/in* spring, at two different bit diameters. The periodic oscillations are initiated once per revolution and are due to the initial bottom hole geometry.

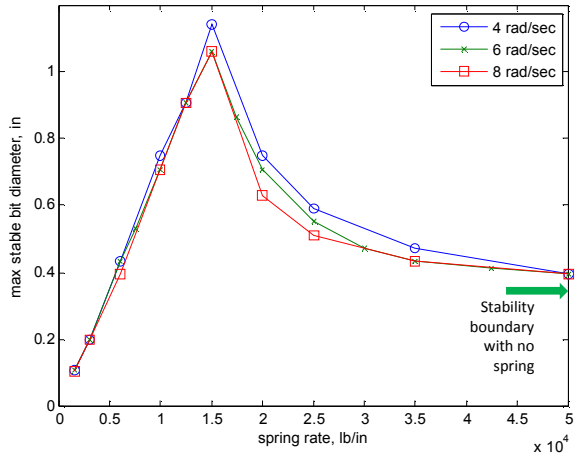

Figure 5. Maximum stable bit diameter *a* versus variable spring rate k_{vs}.

drilling: 4, 6, and 8 *rad/sec*. The maximum stable values are plotted in Fig. 5. To establish a baseline for stability, the same process was repeated for a system with only the Upper Drillstring Admittance and Rock/Bit Impedance - i.e. with the Lower Drillstring and Variable Spring blocks removed entirely from Fig. 2. For all three speeds, the baseline stability limit was approximately 0.35". The limiting bit diameters are smaller than expected, likely because the model does not include nonlinearities. The *relative* stability of different k_{vs} values, rather than physically perfect modeling, is our primary interest in this work. Fig. 5 indicates the following interesting results:

- Stability boundaries are only marginally impacted by angular velocity, with lower speeds slightly more stable.
- At large values of k_{vs}, the stability limit converges close to the baseline (no spring) limit, as expected.
- Intermediate stiffness values are the most stabilizing, increasing the stable bit radius by 3x versus baseline. This provides strong support for the rationale of using a variable spring. Simply making the system as soft as practical is ill-advised. The advantage of intermediate stiffness values also aligns with some prior published experimental data, e.g. Fig. 14 in [7].
- At the lowest stiffness values, the spring is significantly destabilizing; stability is worse than with no spring at all.

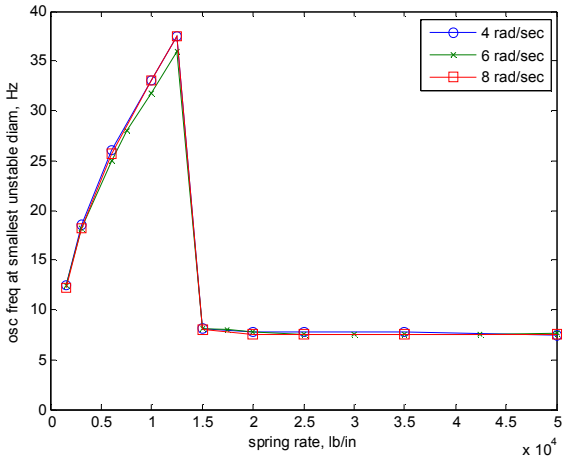

Figure 6. Vibration frequency at minimum unstable radius *a* versus k_{vs}.

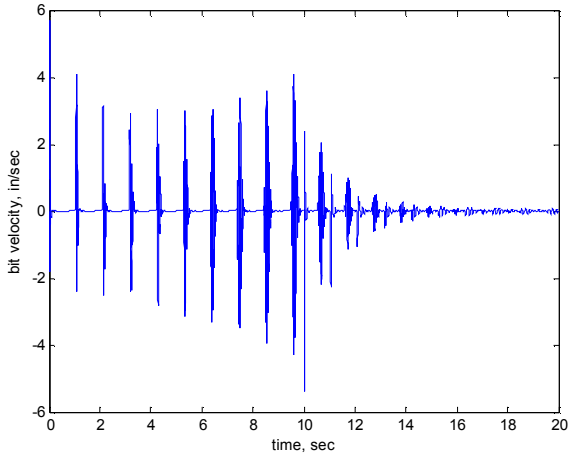

Figure 7. Bit velocity for simulation at ω=6 r/s, 0.51" diameter. Stiffness k_{vs} switches at t=10 sec from 6k *lb/in* to 15k *lb/in*.

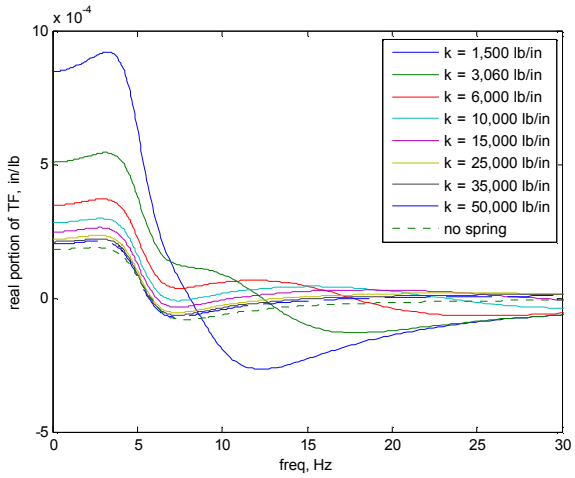

Figure 8. Real portion of net system transfer function.

Furthermore, the shape of the plot suggests two distinct stability limits, one dominating at low stiffness and another at high stiffness. Fig. 6 plots the vibration frequencies at the minimum unstable *a* for each stiffness tested, and confirms that there are two distinct characteristics of instability, which bifurcate depending on the value of k_{vs}. At low k_{vs}, the frequencies of unstable vibrations are roughly proportional to the natural frequency of the variable spring module, indicating that the instability is attributed to the new mode introduced by this module. At higher k_{vs}, the unstable frequencies are virtually independent of k_{vs}, and align closely with the oscillation frequency of the upper drillstring when interacting with the rock directly (~7.5 *Hz*). Note that the interaction with the effective stiffness of the rock results in vibrations at a higher frequency than the resonant frequency of the SHO alone (~5.25 *Hz*).

IV. Implications for Downhole Control

From Fig. 5 it is clear that to minimize unstable self-excited vibrations for this particular example, it is best to select a spring rate around 15k *lb/in*. From Fig. 6, this is also the minimum stiffness that avoids introducing its own instabilities. Fig. 7 shows the bit velocity as k_{vs} is changed from a destabilizing value (6k *lb/in*) to a stabilizing value (15k *lb/in*) at time = 10 s. The unstable vibrations are rapidly suppressed by the appropriate spring.

For control, the key challenge is identifying this optimal stiffness in situ, with only measurements available at the variable spring module, in order to avoid telemetry in the control loop. However, while the dynamics of the rock/bit interaction (e.g. the properties of the rock and the changing characteristics of the cutters as they wear) are difficult to estimate while drilling, they significantly impact both the vibration frequencies and the stability of various modes.

Per [3], stability of particular modes (and their resistance to self-excited vibrations) may be improved by boosting the real portion of the transfer function between the force and displacement at the bit, $G=Z_{bit}/F_{bit}$, at problematic frequencies. This enables potential concepts for controlling the variable stiffness based only on the measured frequency content of vibration, and a dynamic model of the drillstring, without requiring knowledge of the rock/bit dynamics.

Fig. 8 plots *Re(G)* for the simulated system with various spring rates. At the highest stiffness values, the transfer function approaches that of the system with no vibration absorber, as expected. From Fig. 6, destabilizing vibrations occur around 7.5-8 *Hz* in this regime, and in Fig. 8 it is clear that *Re(G)* is negative in this range. The lower stiffness values significantly boost *Re(G)* at low frequencies, but they drive it negative at slightly higher frequencies – hence there are instabilities in the 12-38 *Hz* range (Fig. 6). While it is by no means obvious from Fig. 8 which stiffness value is optimal, it is certainly plausible that the intermediate stiffness values in the 10k-25k *lb/in* range provide sufficient help at frequencies <10 *Hz* without dramatically compromising higher frequencies. Thus the fact that these springs are the most stabilizing agrees with the model in [3].

One could imagine sculpting a controller that optimizes the curve plotted in Fig. 8, for instance to maximize the minimum value of *Re(G)* over a broad range of frequencies believed to be most relevant to drilling conditions. However, to implement control based on *Re(G)* would require a model of the full drillstring dynamics. As noted, these dynamics vary greatly from interactions with the wellbore, and cannot in general be accurately determined based on a priori models. One possibility is to perform real-time system identification downhole. This is difficult because of measurement noise and a lack of rich, broadband excitation.

Another potential approach is to select variable spring stiffness based on the measured vibrations and the properties of the real portion of the transfer function for only G_l and A,

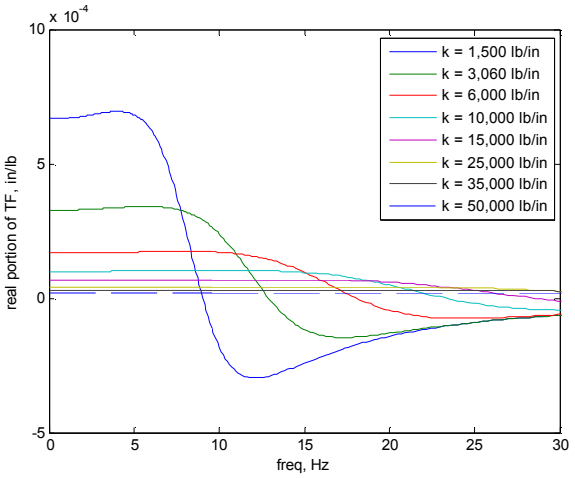

Figure 9. Real portion of VRS module transfer function.

which can both be accurately known if A is close to the bit and G_l is simple. In the structure of Figs. 1 and 2, a composite transfer function G_{lA} would replace the G_l (lower drillstring) and A (variable spring) blocks, and would be a mixed-causality two-port, appearing as an admittance to the bit and an impedance to G_u (upper drillstring). The relationship between G_{lA} and $Re(G)$ is complex and depends on G_u. However, our example suggests that analysis of $Re(G_{lA})$ may provide hints that could enable the impact of adding these dynamics to the system to be estimated.

For the example, G_{lA} is the transfer function for a spring-mass-damper, and $Re(G_{lA})$ is plotted in Fig. 9 for the same values of k_{vs}. To reduce self-excited vibrations, adding G_{lA} must boost $Re(G)$ in problematic frequency ranges. In this example, it appears that the frequency ranges at which a particular G_{lA} boosts $Re(G)$ may be inferred from features of $Re(G_{lA})$. Specifically, the downward zero crossings of $Re(G_{lA})$ (Fig. 9) occur at frequencies that are quite close to the frequencies at which the curves for $Re(G)$ with corresponding k_{vs} intersect the original $Re(G_u)$ curve with no spring (Fig. 8). For example, with a stiffness of 1,500 *lb/in*, the zero crossing (Fig. 9) occurs at ~9 *Hz*, as does the intersection between the 1,500 *lb/in* and "no spring" curves in Fig. 8. The intersection points similarly align for other stiffnesses, generally within 10% in frequency.

This is just a single example, and needs to be studied further. If this pattern holds, however, it suggests that it may be feasible to *estimate* the frequency range at which a particular spring will boost $Re(G)$ based only on the known dynamics of G_l and A. If true in general, this could facilitate effective local controllers that work via the following steps:

1. Continuously measure downhole vibrations, and analyze frequency content (e.g. via power spectral density).
2. Identify frequencies that contain power over a threshold. Store in memory that forgets over a period of time.
3. Select spring rate that optimizes benefit across the frequencies with observed powerful vibrations. For example, select a rate that maximizes the minimum boost to $Re(G)$ across the set of frequencies.
4. Repeat continuously.

V. Discussion and Conclusions

The work presents and demonstrates a new modeling framework for drillstrings with autonomously controllable dynamic modules for suppression of self-excited vibrations. Results align with previous experiments and provide insight into the relationships between stiffness, stability limits, and frequencies of unstable vibration in drillstrings. The results suggest interesting directions for further study to develop controllers to tune stiffness to suppress vibrations.

Significant additional work is required to develop, validate, and ultimately realize autonomous downhole controllers. Further simulations and analysis are required to determine whether the trends reported in Sections III and IV generalize to systems of higher dynamic order. This work must be accompanied by controlled experiments. Sandia's Hard Rock Drilling Facility is well suited to this work, and our team has developed a laboratory prototype Variable Rate Spring [8]. Experimental studies will require overcoming several challenges, including: nonlinearities that, among other things, prevent unstable vibrations from growing indefinitely; as well as resonant (but stable) vibrations that can be difficult to distinguish from truly unstable self-excited vibrations. Prior to deployment, suitable signal processing and real-time control algorithms must be developed and implemented on rugged hardware suitable for downhole use – a significant challenge in its own right.

References

[1] D. Reid and H. Rabia, "Analysis of drillstring failures," in *Proc. SPE/IADC Drilling Conf.*, Amsterdam, Netherlands, 1995.

[2] L.W. Ledgerwood et al., "Downhole vibration measurement, monitoring, and modeling reveal stick/slip as primary cause of PDC-bit damage in today," in *Proc. SPE Ann. Tech. Conf.*, Florence, 2010.

[3] D. Dareing, J. Tlusty and C. Zamudio, "Self-excited vibrations induced by drag bits," *J. Energy Res. Tech.*, vol. 112, pp. 54-61, 1990.

[4] S. Wu et al., "Identifying the root cause of drilling vibration and stick-slip enables fit-for-purpose solutions," in *Proc. IADC/SPE Drilling Conf. Exh,*, San Diego, CA, 2012.

[5] Y.S. Tarng, T.C. Li and M.C. Chen, "On-line drilling chatter recognition and avoidance using an ART2-a neural network," *Intl. J. Machine Tools and Manufacture*, vol. 34, pp. 949-957, 1994.

[6] S. Ema and E. Marui, "Theoretical analysis on chatter vibration in drilling and its suppression," *J. Mat. Proc. Tech.*, vol. 138, pp. 572-578, 2003.

[7] D.W. Raymond and M.A. Elsayed, "Controllable magneto-rheological fluid-based dampers for drilling," U.S. Patent 7,036,612, 2006.

[8] D.W. Raymond et al., "Active suppression of drilling system vibrations for deep drilling," Sandia National Laboratories report SAND2015-9432, October, 2015.

[9] D. de Klerk, D.J. Rixen and S.N. Voormeeren, "General framework for dynamic substructuring: History, review, and classification of techniques," *AIAA Journal*, vol. 46, pp. 1169-1181, 2008.

[10] E. Detournay and P. Defourny, "A phenomenological model of the drilling action of drag bits," *Intl. J. Rock Mech. Min. Sci.*, vol. 29, pp. 13-23, 1992.

[11] E. Detournay et al., "Drilling response of drag bits: theory and experiment, *Intl. J. Rock Mech. Min. Sci.*, vol. 45, pp. 1347-60, 2008.

[12] D.W. Raymond et al., "Laboratory simulation of drill bit dynamics using a model-based servo-hydraulic controller," *J. Energy Res. Tech.*, vol. 130, pp. 54-61, 2008.

[13] N. Hogan and S. Buerger, "Impedance and interaction control," in *Robotics and Automation Handbook*, T. Kurfess, Ed., New York: CRC Press, p. 19-1.

[14] N. Hogan, "Impedance control: An approach to manipulation," *J. Dyn. Sys. Meas. Ctrl.*, vol. 107, pp. 1-24, 1985.

[15] J. Tlusty, "Manufacturing processes and equipment," *IIE Trans.*, vol. 34, p. 647, 2000.

[16] F.E. Dupriest and W.L. Koederitz, "Maximizing drill rates with real-time surveillance of mechanical specific energy," in *Proc. SPE/IADC Drilling Conf.*, Amsterdam, Netherlands, 2005.